Biophys Struct Mech (1984) 10 : 257–273

Biophysics of Structure and Mechanism

Determination of the Raman Tensor of the Haem Group in Myoglobin by Resonance Raman Scattering in Solution and Single Crystals

S. el Naggar, R. Schweitzer-Stenner, W. Dreybrodt, and A. Mayer

Universität Bremen, Fachbereich 1 – Physik, D-2800 Bremen 33, Federal Republic of Germany

Abstract. We have measured the depolarization ratio and the excitation profiles of the Raman lines at 1,355 cm^{-1}, 1,564 cm^{-1} and at 1,373 cm^{-1}, 1,580 cm^{-1} in solutions of *deoxy*Mb and ferric MbCN, respectively, in the region between the Soret and the α, β-bands. From their dispersion we have determined the tensor components of the Raman tensor by an extension of Loudon's theory, taking into account static distortions from the ideal D_{4h}-symmetry of the haem group, induced by haem-protein interactions and the interaction of the side-chains with the porphyrin skeleton (Schweitzer et al. 1984).

Analogous to the excitation profiles in solution, measurements on Mb single crystals yield intensities $I_{a,b}$ which are related to the tensor components viewed in the laboratory system, spanned by the three orthogonal crystals axes *a, b, c**. By using the structural data of the crystals and coordinate transformation from the system of the molecular coordinates into the laboratory system, the quantities $I_{a,b}$ can be calculated by use of the tensor components determined from the solution data.

The values thus calculated and those which are determined experimentally from the single crystals are in good agreement. This confirms the theoretical approach of Schweitzer et al. (1984).

Key words: Myoglobin – Resonance Raman scattering – Dispersion of depolarization ratio – Symmetry distortions – Haem – Single crystals

Introduction

Schweitzer et al. (1984) have reported measurements of the depolarization ratio (DPR) dispersion and the excitation profiles (EPS) of the 1,355 cm^{-1} Raman line of deoxyhaemoglobin (*deoxy*Hb) in the frequency region between Soret and α, β-band. Starting from the theoretical treatments of Loudon (1979), Peticolas et al. (1970), and Collins et al. (1973) they formulate the polar-

izibility tensors as a linear combination of tensors due to the Raman active modes, which transform like A_{1g}, B_{1g}, B_{2g}, and A_{2g} in D_{4h}-symmetry. The coefficients of the tensors have been related to symmetry-classified static distortions of the haem group from its ideal D_{4h}-symmetry, which are caused by the side chains of the haem pyrrol rings, the covalent Fe^{2+}-His (F8) bond between the haem and the globular protein and the haem-apoprotein interaction. With this approach the DPR curves and the EPS were fitted simultaneously with one set of constants. They justified the reliability of their approach by the fact that one physically meaningful and interpretable set of constants could explain simultaneously three different experimental sets of data. In view of the consequences of this new method, which can be used to detect static distortions of the haem group due to solvent-protein-chromophore interaction, an independent check appears to be valuable for further confirmation. If the theoretical approach of Schweitzer et al. (1984) is correct, one is able to obtain all the components of the Raman tensor in the frequency range between the α, β- and the Soret bands by fitting the experimental data of the DPR and EPS to the theory. Any data for different Raman scattering experiments are then predictable at least in this frequency range. We have therefore performed resonance Raman scattering in both solutions and single crystals of ferric MbCN and *deoxy*Mb. For the solution conditions, we have determined EPS and DPR. For single crystals, we have measured on *a, b*-planes the four excitation profiles, which result from the possible orientations of polarization of exciting and scattering light along the *a, b*-axes of the crystal.

By fitting the DPR and EPS obtained from the solution data, we obtain the Raman tensor, which is used to calculate the four EPS of the crystal. With this method seven independent sets of experimental data should be described by one common set of parameters, obtained from the solution data.

Especially good candidates for this procedure are the lines at 1,355 cm^{-1} and 1,564 cm^{-1} in *deoxy*Mb and the corresponding lines in ferric MbCN, since their DPR and EPS do not show, in the limits of accuracy, any changes resulting from the pH of the solution, in contrast to Hb (Schweitzer et al. 1982).

This leads us to the assumption that both in solution and crystal the molecules exhibit the same properties. From this we may assume that the Raman tensor components of the molecule are the same in both solution and crystal. This assumption of the oriented gas-phase model of the crystal seems to be realistic, since our findings show that both, in *deoxy*Mb and ferric MbCN crystals, the four different excitation profiles obtained in the scattering geometries $\bar{c}^*$ (a, a) c^*, $\bar{c}^*$ (a, b) c^*, $\bar{c}^*$ (b, a) c^*, and $\bar{c}^*$ (b, b) c^* are in good agreement with the values predicted from the Raman tensor, which was obtained from DPR and EPS of the corresponding solutions.

From these measurements of Raman scattering of the haem chromophore in single crystalline *deoxy*Mb and ferric MbCN, reported for the first time in this paper, we can draw two main conclusions:

a) The model of Schweitzer et al. (1984) is confirmed since the set of crystalline and solution data can be related to one common Raman tensor.

b) There is no change in the molecular structure configuration of the chromophore in solution and crystalline state for *deoxy*Mb and ferric MbCN.

In the first part of the following description we discuss the relation of the Raman tensor β_{ik} to the DPR and EPS of the molecule in solution and the theoretical approach of Schweitzer et al. (1984), from which by a fitting procedure to the experimentally obtained DPR and EPS, the components β_{ik} of the Raman tensor are calculated.

In the second part, by using the oriented gas-phase model for the crystal, we show the experimentally determined excitation profiles are related to the components of the Raman tensor. This relation is determined by the directional cosines between the axes defined by crystal and those defined by the Raman tensor of the molecule. The molecular axes are determined within a narrow range by considering the polarization properties of absorption of light polarized along the three different crystals directions *a, b,* and *c*. Finally the results are presented and discussed.

Relation of Raman Intensities Measured from Solutions to the Raman Tensor in the Molecular Coordinate System

In solutions three significant quantities can be measured. These are the excitation profiles $I_\parallel$ and $I_\perp$ and the depolarization ratio ϱ. They are related by Placzek's (1934) polarizibility theory (Sushchinskii 1972) to the invariants of the Raman tensor by

$$\begin{aligned} I_\parallel &= \frac{I_\parallel^{\text{obs}}}{I_0 \tilde{\nu}_R^4} = A(3\gamma^2 + 5\beta^a) \\ I_\perp &= \frac{I_\perp^{\text{obs}}}{I_0 \tilde{\nu}_R^4} = A(10\beta^s + 4\gamma^2) \\ \varrho &= \frac{I_\parallel}{I_\perp} = \frac{3\gamma^2 + 5\beta^2}{10\beta^s + 4\gamma^2}. \end{aligned} \tag{1}$$

$I_\parallel^{\text{obs}}$ and $I_\perp^{\text{obs}}$ are the observed Raman intensities, if the exciting laser light is polarized normally to the scattering plane and the scattered light is polarized parallel or normally to the scattering plane, respectively. I_0 is the intensity of the exciting radiation. $\tilde{\nu}_R$ is the scattered Raman frequency. The tensor invariants γ^2, β^s, β^a are defined in the article by Schweitzer et al. (1984). A is a constant indicating that our data are taken in arbitrary units. The relations in Eq. (1) are valid only if the solution is fully transparent to the exciting and scattered radiation. In the case of absorbing material like Mb corrections are necessary.

In our experimental set-up, however, only a scattering volume of a depth of 0.3 mm was imaged into the spectrometer. If one uses diluted solutions of 10^{-4} mol/l the absorption of the radiation in this small path length can be neglected and to an accuracy of a few percent no corrections are necessary.

Calculation of the Components of the Molecular Raman Tensor from the Solution Data

Extending the Loudon-theory (1979) of the Raman tensor by transitions to the first vibronically excited sublevel of the electronic states from the 0-sublevel of the electronic ground state and including symmetry-classified static distortions from the ideal D_{4h}-symmetry using Collin's et al. (1973) approach, Schweitzer et al. (1984) obtained the following expression for the tensor of polarizibility:

$$(\hat{\beta})_{\text{dist}} = \alpha_{QB}^{A_{2g}} \hat{\Gamma} A^{2g} \{F_{QB}^{\vec{a}}(\tilde{\nu}_Q, \tilde{\nu}_B) + C_{QB}^{\vec{a}} F_{QB}^{\vec{a}}(\tilde{\nu}_Q + \tilde{\nu}_\mu, \tilde{\nu}_B + \tilde{\nu}_\mu)\}$$
$$+ \sum_{e,s} \left\{ \left[\sum_{\Gamma} \alpha_{es}^{\Gamma} \hat{\Gamma}^{\Gamma} \right] [F_{es}^{\vec{s}}(\tilde{\nu}_e, \tilde{\nu}_s) + C_{es}^{\vec{s}} F_{es}^{\vec{s}}(\tilde{\nu}_e + \tilde{\nu}_\mu, \tilde{\nu}_s + \tilde{\nu}_\mu)] \right\} \quad (2)$$

e, s are related to the excited states Q and B, which are responsible for the optical transitions at $\tilde{\nu}_Q$ and $\tilde{\nu}_B$.

$\tilde{\nu}_\mu$ is the energy of a representative phonon, leading to vibronic sidebands in the Q and B transitions.

$F_{es}^{\vec{a},\vec{s}}$ are frequency functions due to the electronic structure of the haem. The quantities α_{es}^{Γ} are complex constant for each tensor $\hat{\Gamma}^{\Gamma}$ of the representation Γ tabulated by McClain (1971) for D_{4h}-symmetry. $C_{es}^{\vec{s},\vec{a}}$ is related to Franck-Condon overlap integrals and vibronic coupling of the Q and B state and results from considering contributions due to transitions into the vibronic sideband (Schweitzer et al. 1984).

We use Eq. (2) and Eq. (1) to fit the DPR dispersion curves of the oxidation marker line at 1,355 cm^{-1} and of the spin-marker-line at 1,564 cm^{-1} of *deoxy*Mb and the corresponding lines of ferric MbCN-solutions simultaneously with the corresponding excitation profiles in solution. From these fits one obtains the complete frequency-dependent polarizibility tensors of the two Raman lines in the molecular system. These are used to calculate the EPS obtained from the measurements on the crystals as described in the following section.

Relation of Raman Intensities Measured on Crystals to the Components of the Raman Tensor in the Molecular Coordinate System

The following treatment is based on the general theory of Raman scattering as described for instance by Sushchinskii (1972). The dipole moment $\vec{\mathbf{P}}$ induced in an electronic system by the exciting electromagnetic wave, with electric field vector $\vec{\mathbf{E}}$ is related to the tensor of polarizibility $\hat{\beta}$ in the coordinate system of the molecule by

$$P_i = \sum_k \beta_{ik} E_k , \quad (3)$$

where i, $K = x, y, z$ are the coordinates of the molecular reference system, E_k, P_i are the components with respect to the corresponding axes in the molec-

ular coordinate system. β_{ik} are the components of the Raman tensor $\hat{\beta}$. In the Mb single crystal in a first step we consider one haem chromophore being fixed in the spatial coordinate system given as laboratory system, which is described by the *a*, *b*, and *c** axes of the crystal.
We choose $a = X$-axis, $b = Y$-axis, $c^* = Z$-axis.

The dipole moment $\vec{\mathbf{P}}'$ viewed in this coordinate system is obtained by transformation of $\vec{\mathbf{P}}$ in the molecular system into the laboratory system by

$$P'_L = \sum_M E'_M \beta'_{LM} \tag{4}$$

with

$$\beta'_{LM} = \sum_{i,k} n_{iL}\, n_{kM}\, \beta_{ik}\,. \tag{5}$$

β'_{LM} is the scattering tensor in the laboratory system. $L, M = X, Y, Z$. n_{iL} and n_{kM} are the direction cosines of the angles between axes i, L, and k, M of the molecular system and the laboratory system respectively.

For our particular scattering geometry, which is given in the notation of Damen et al. (1966) by $\bar{Z}(X, X)\, Z$, $\bar{Z}(X, Y)\, Z$, $\bar{Z}(Y, X)\, Z$, and $\bar{Z}(Y, Y)\, Z$, the intensity of radiation scattered into the solid angle $d\Omega$ is given by Sushchinskii (1972)

$$dI = 4\,\pi^3 c \tilde{\nu}_s^4 [P'_x P^{*'}_x + P'_y P^{*'}_y] \cdot d\Omega = dI_x + dI_y\,. \tag{6}$$

This sum is composed of two components polarized in the X and Y direction respectively. These two components dI_X and dI_Y are the quantities to be measured. $\tilde{\nu}_s$ is the frequency of the scattered light.

To obtain the quantities n_{iL} and n_{kM} we have to define the molecular coordinate system with respect to the crystal coordinate system. This will be done in a later section of this paper.

In the second step we have to consider that the unit cell of the monoclinic form (type A) crystal of Mb contains two Mb molecules related to each other by a screw axis (*b*-axis) of twofold symmetry (Bennet et al. 1961; Eaton and Hochstrasser 1968; Kendrew and Parrish 1956). We have to deal therefore with two different arrays of haem groups in the crystal. We denote these with subscripts 1 and 2.

Since the electronic transitions of Mb to the Soret band and the α-band result from $[(a_{1u}, a_{1u}) \rightarrow (a_{1u}, e_g)$ and $(a_{2u}, a_{2u}) \rightarrow (a_{2u}, e_g)]$ electronic transitions, they are x, y polarized with respect to the molecular frames (Eaton and Hochstrasser 1968; Churg and Makinen 1978).

In the region of the Ar^+-laser only the dipole moments of these transitions contribute to Raman scattering. Therefore the Raman tensor simplifies to a two by two tensor, since all components $\beta_{i,k}$ with either $i = Z$ or $k = Z$ may be neglected.

Equation (5) can now be reformulated with only four tensor components as

$$\hat{\beta}' = \hat{A}\hat{\beta}\,, \tag{7}$$

where the Raman tensors $\hat{\beta}$, $\hat{\beta}'$ are written for convenience as vectors

$$\hat{\beta} = (\beta_{xx}, \beta_{xy}, \beta_{yx}, \beta_{yy}) . \tag{7a}$$

$\hat{A}$ is a matrix constituted of the products of the directional cosines according to Eq. (5)

$$a_{iL}a_{kM} = n_{iL}n_{kM} . \tag{7b}$$

In our particular scattering geometry (back scattering) the exciting radiation and the Raman radiation propagate parallel to the Z-axis, and are polarized parallel to either the X- or Y-axis of the crystal. Therefore four measurable intensities (crystal-EPS) I_{XX}, I_{XY}, I_{YX}, and I_{YY} result. They are obtained by incoherent superposition of the scattering intensities of the two different arrays of haem groups in the crystal using Eq. (6) and Eq. (4)

$$I_{LM} = 4\,\pi^3 c\tilde{\nu}_s^4(\beta'^{(1)}_{ML}\beta'^{(1)*}_{ML} + \beta'^{(2)}_{ML}\beta'^{(2)*}_{ML})E_L^2\frac{N}{2}(\delta\Omega) . \tag{8}$$

$L, M = X, Y$. N is the number of molecules participating in the scattering process, and E_L^2 relates to the intensity of the exciting radiation. The indices (1) and (2) refer to the two arrays of haem groups.

The directional cosines of array 1 and array 2 are related to each other by the geometrical properties of the crystal lattice (Kendrew and Parrish 1956). This leads to the relations

$$n_{iL}^{(1)} = -\,n_{iL}^{(2)} \text{ if } L = X, Z$$

$$N_{iL}^{(1)} = +\,n_{iL}^{(2)} \text{ if } L = Y .$$

Introducing this properties into Eq. (7) we obtain

$$\beta'^{(1)}_{ML}\beta'^{(1)*}_{ML} = \beta'^{(2)}_{ML}\beta'^{(2)*}_{ML} = \beta'_{ML}\beta'^{*}_{ML} .$$

The EPS measured from the crystal are now defined analogous to those measured from solutions as

$$|\beta'_{ML}|^2 = \frac{I_{LM}}{E_L^2\,4\,\pi^3 c\tilde{\nu}_s^4 N(\delta\Omega)} = \frac{I_{LM}\cdot A_c}{\tilde{\nu}_s^4 I_0} . \tag{9}$$

A_c is a constant indicating arbitrary units.

The $\beta'_{ML}\beta'^{*}_{ML}$ are proportional to the measured intensities $I_{L,M}$ and can be calculated from Eq. (5) or Eq. (7) respectively. Equation (8) refers to the case of an ideally transparent crystal, which does not absorb either the incident or the scattered radiation. Mb-crystals, however, are absorbing light dichroically (Kendrew and Parrish 1956; Bennet et al. 1961; Eaton and Hochstrasser 1968; Churg and Makinen 1978) and therefore corrections are necessary.

In the case of strongly absorbing crystals, i.e., when the penetration depth of light into the crystal is small compared to the length of the scattering volume,

imaged into the monochromator, Loudon (1965) has given the following relation between the observed intensity I_{LM}^{obs} of Raman scattering and the intensity I_{LM} that would be observed in a non-absorbing crystal.

$$I_{LM}^{\text{obs}} = \frac{I_{LM}}{\varepsilon_L(\tilde{\nu}_L) + \varepsilon_M(\tilde{\nu}_s)} . \tag{10}$$

For our experimental set-up a volume of length of 0.3 mm along the optical axis is imaged into the monochromator.

In the strongly absorbing crystal the penetration depth is large compared to this and Loudon's expression holds. Using Eq. (9) and Eq. (10) we finally obtain the following relation between the observed Raman intensities and the coefficients of the Raman tensor in the crystal coordinate system.

$$|\beta'_{ML}|^2 = \frac{A_c I_{LM}^{\text{obs}}}{I_0 \tilde{\nu}_s^4} [\varepsilon_L(\tilde{\nu}_L) + \varepsilon_M(\tilde{\nu}_s)] . \tag{11}$$

The extinction coefficients $\varepsilon_L(\tilde{\nu})$ have been measured using a Leitz microphotometer. Since the $\varepsilon_L(\tilde{\nu})$ are also important in determining the z-direction of the Raman tensor the results will be discussed in the next section.

Experimental

a) Material

Myoglobin (Mb) from sperm whale was commercially obtained in a lyophilized form (Miles). Crystals were grown according to the procedure described by Kendrew and Parrish (1956). Solid Mb was dissolved in water and dialysed against distilled water at 4° C, then centrifuged in order to remove denatured material. To small aliquots of Mb solution of about 1.0 mM concentration, saturated $(NH_4)_2SO_4$ solution was added in such amount as to establish pH-values in the range between 6.5 and 7.3. Crystallization proceeds during several days or even weeks depending on the solution conditions. This procedure yields aquomet Mb single crystals of monoclinic form, type A, flattened on the $a \times b$ face [001] or $b \times c$ face [100].

The crystallographic axes a and b were determined optically with the aid of a polarization microscope. Crystals had the following dimensions. a-axis: 3–4 mm; b-axis: 1–2 mm; c-axis: 0.1–1 mm. The crystals were placed between plates of quartz with a drop of mother liquid [2–3 M $(NH_4)_2SO_4$] and mounted on a goniometer.

Crystals of *deoxy*Mb were obtained by addition of $Na_2S_2O_4$ to aquomet-Mb crystals under nitrogen atmosphere. Crystals of cyanomet-Mb were obtained by addition of KCN to aquomet-Mb crystals. The purity of the derivatives of Mb was checked by the optical absorption spectra.

Solutions of Mb were prepared by diluting aquomet-Mb crystals in bidistilled water or buffer. The pH-value of the Mb solutions were adjusted by dialysis

against 0.4 M *tris* and *bis-tris* buffer. Solutions of *deoxy*Mb were prepared by addition of $Na_2S_2O_4$ to aquomet-Mb solution in presence of N_2 atmosphere.

b) Method

Measurements of RR-scattering were performed with an Ar-Ion laser using a Spex-spectrometer as described by Schweitzer et al. (1982).

The measurements on crystals were done in back-scattering geometry. The scattered light was observed at angle of 180° to the direction of the incident light, the incident beam being perpendicular to the *a-b* face of the Mb single crystal and being either polarized parallel to the *a*-axis or to the *b*-axis. The scattered light was analyzed with the aid of a polarizer parallel to the *a*- or *b*-axis. The exact alignment of the polarization direction of the exciting light and the scattered light to the crystal axes *a* or *b* was achieved by the following procedure. In a first step by rotating the polarization direction of the laser beam, the transmission direction of the analysing polarizer and the *E*-vector of the exciting light were set exactly parallel. The deviation of this direction from the *a*-axis of the crystal amounted then to a few degrees. In this position the Raman signal was measured in the geometry $\bar{C}$ $(a, a)C^*$. Then both the direction of the exciting *E*-vector and the polarizer were changed by the same amount until an extremum of the scattered intensity was obtained. As can be shown easily by calculation of the Raman intensities of the two arrays of haem planes in the laboratory coordinate system, this is exactly the condition for perfect parallelism between the crystal axis-*a* and the exciting light vector. In order to eliminate the different transmission of the spectrometer for the two different polarization components of scattered light, a polarization scrambler was placed between polarizer and entrance slit. The measurements were performed at room temperature. The crystal could be exposed up to 50 mW power of the laser and no variations of its physical and chemical properties could be detected. The measurements on solutions of Mb were done also in a back-scattering geometry, using a sample container of quartz with plane faces situated in a copper block for cooling (to 4° C). The observed intensities were corrected for the spectral transfer of the spectrometer system.

Results and Discussion

a) Results

We have measured in solutions the excitation profiles as defined in Eq. (1) for the Raman lines at 1,355 cm^{-1} and 1,564 cm^{-1} for *deoxy*Mb. In crystals the corresponding excitation profiles are defined by Eq. (11). Figure 1 shows the experimental results for the line at 1,355 cm^{-1}. The upper part shows the depolarization ratio and the excitation profiles abtained from the solution. The lower part gives the four excitation profiles which were obtained from an *a, b*-crystal surface.

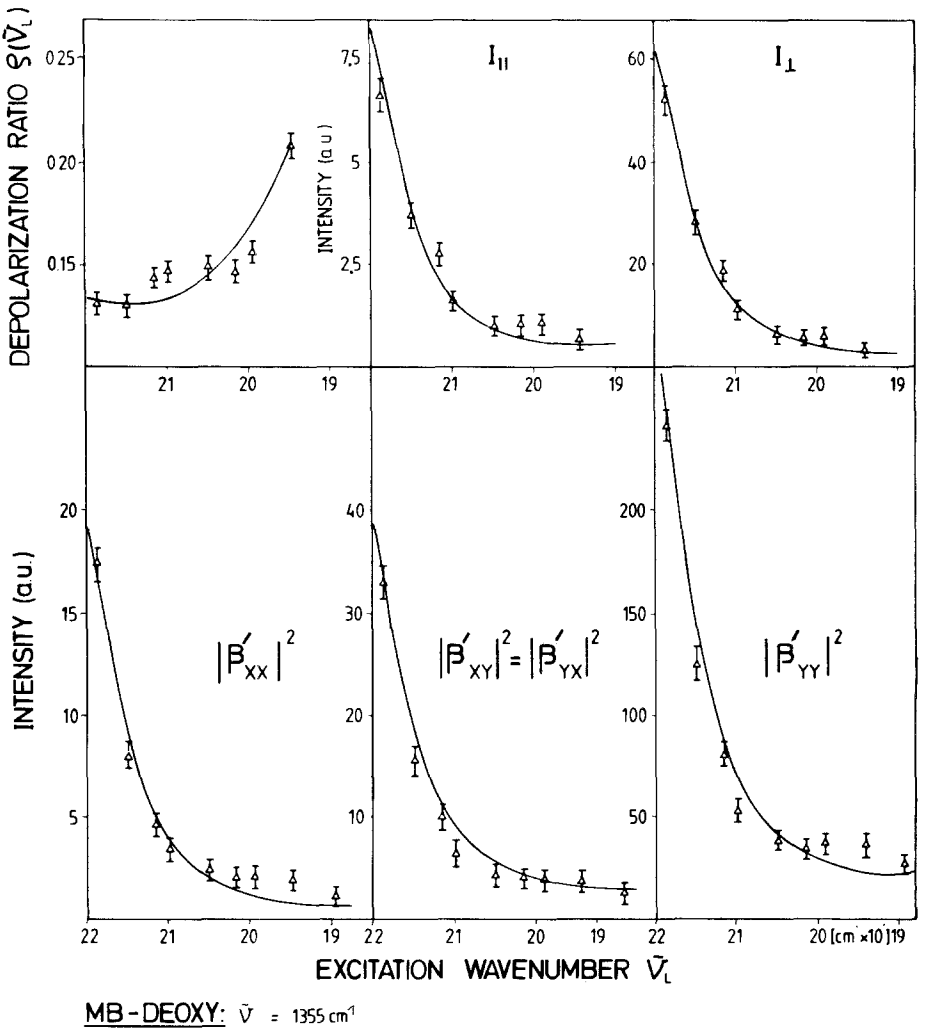

Fig. 1. Depolarization ratio and excitation profiles of the line at 1,355 cm^{-1} in *deoxy*Mb solution (*upper part*) and single crystal excitation profiles (*lower part*). The *full lines* represent the calculated data

Figure 2 shows the corresponding results for the line at 1,564 cm^{-1}. Figures 3 and 4 show the corresponding data of ferric MbCN for the lines at 1,373 cm^{-1} and at 1,580 cm^{-1}.

It is interesting to note that expecially the components $|\beta'_{XY}|^2$ and $|\beta'_{YX}|^2$ show different behaviour in the two different Raman lines. This is due to the fact that the Raman lines at the lower frequency are mainly of A_{1g}-character whereas the higher lines are of A_{2g}-character. The full lines in Figs. 1–4 are calculated by the following procedure. We use the EPS and DPR obtained from the solution and using the method of Schweitzer et al. calculate the fitting constants α^{Γ}_{es}. These are listed in Table 1 for *deoxy*Mb and for MbCN. From

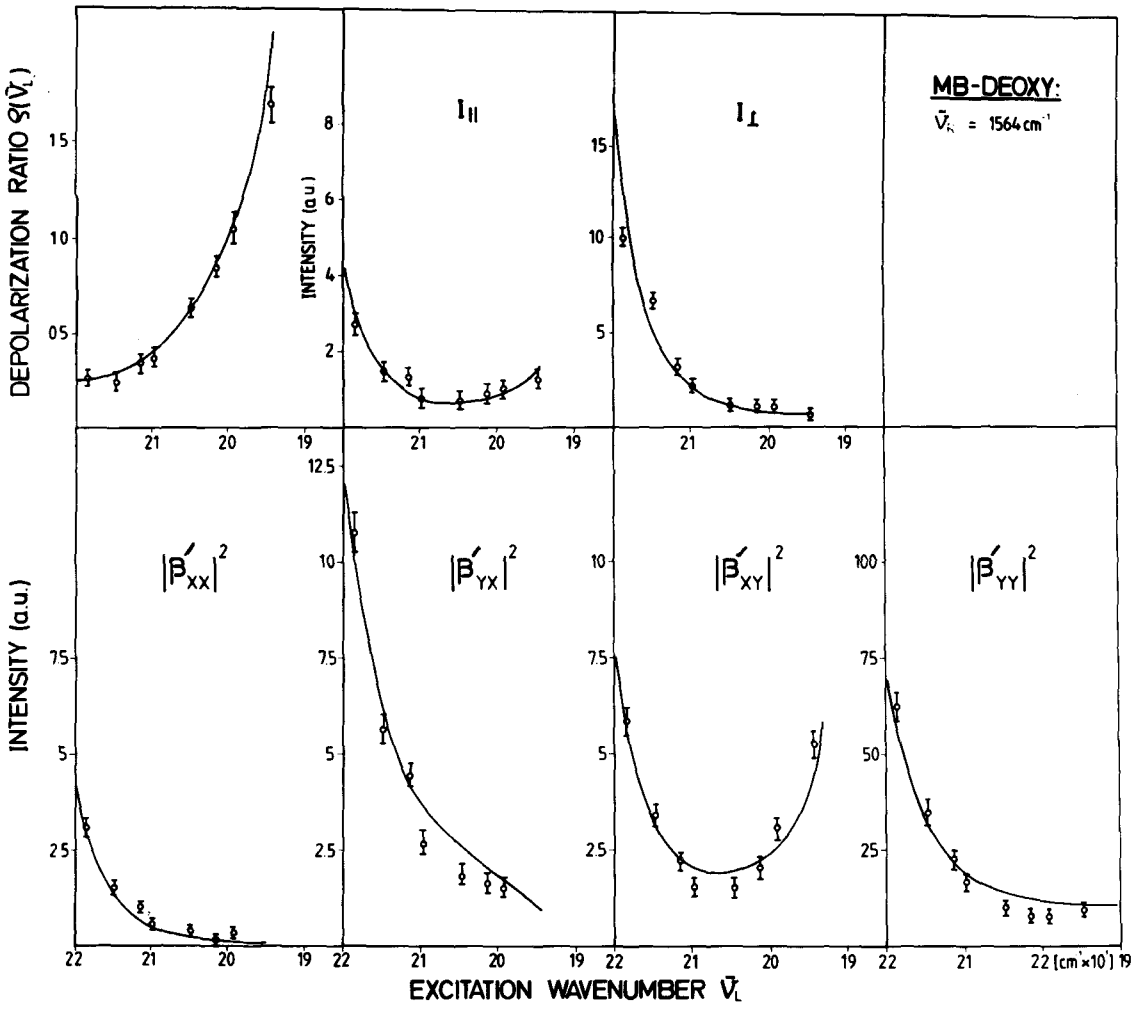

Fig. 2. Depolarization ratio and excitation profiles of the line at 1,564 cm^{-1} in *deoxy*Mb solution (*upper part*) and single crystal excitation profiles (*lower part*). The *full lines* represent the calculated data

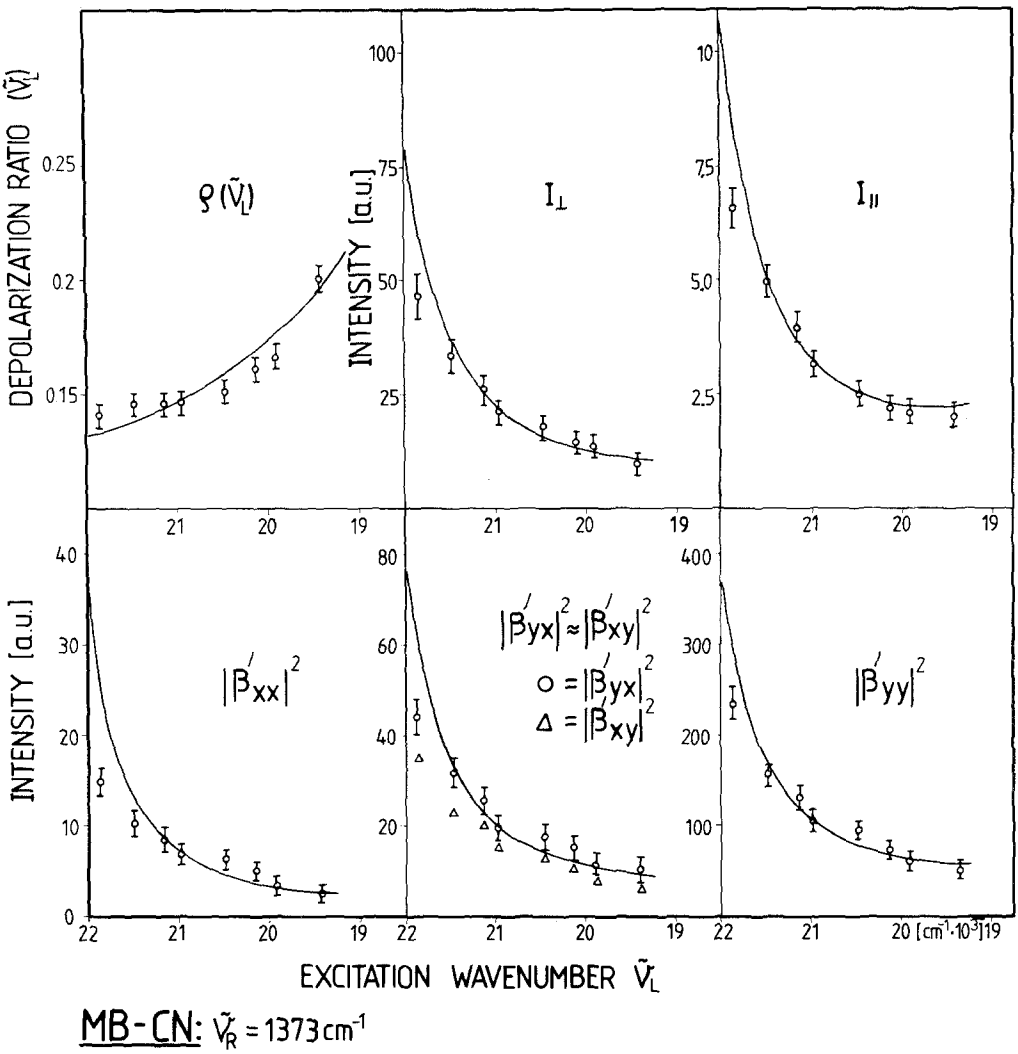

Fig. 3. Depolarization ratio and excitation profiles of the line at 1,373 cm^{-1} in ferric MbCN solution (*upper part*) and single crystal excitation profiles (*lower part*). The *full lines* represent the calculated data

these the Raman tensor in the molecular system can be calculated according to Eq. (2). Using these values and Eq. (7) the values $|\beta'_{LM}|^2$ are calculated and are scaled with one common factor to the experimentally determined values $|\beta'_{LM}|^2$.

For this purpose we have to know the directional cosines n_{iL} of the axes of the molecular coordinate system with respect to the system of the crystal axes *a*, *b*, *c**.

A crude estimation of these directions within an accuracy of about ± 5° can be obtained from the atomic coordinates of the four pyrrol-nitrogen atoms,

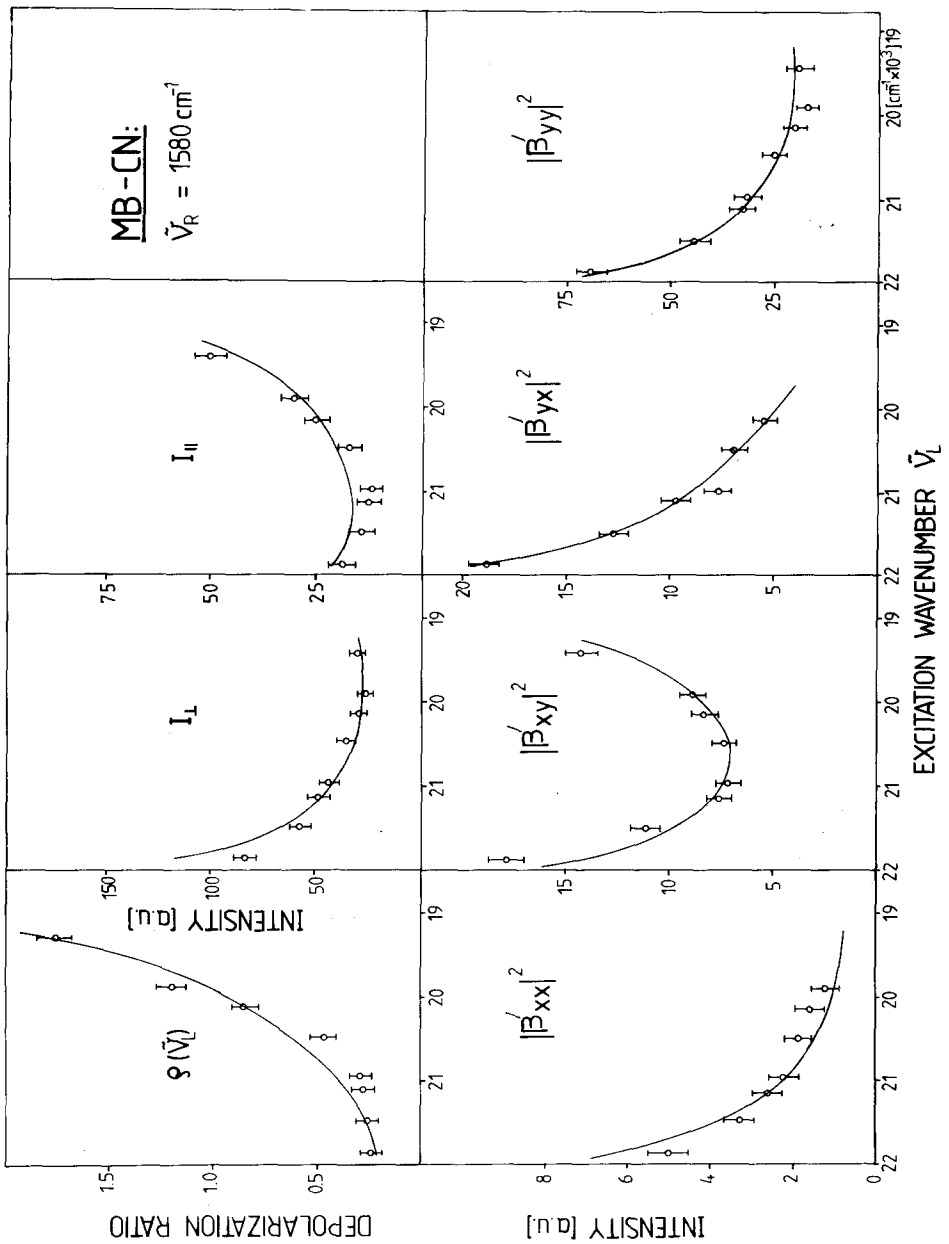

Fig. 4. Depolarization ratio and excitation profiles of the line at 1,580 cm^{-1} in ferric MbCN solution (*upper part*) and single crystal excitation profiles (*lower part*). The *full lines* represent the calculated data

which have been determined by Phillips (1980), Bernstein et al. (1977), and Watson (1969). Since the accuracy of these coordinates is about ± 0.2 Å and furthermore the four nitrogen atoms do not lie coplanar, the z-axis of the Raman tensor cannot be defined unambigously. The directions N_A-N_C and N_B-N_D are also only crude estimates of the x- and y-axes of the molecular system, since they are not orthogonal to each other. A better determination of the z-axis can be obtained if the polarization ratios $\varepsilon_b/\varepsilon_a$ and $\varepsilon_c/\varepsilon_b$ of the extinction coefficients for the x, y polarized Soret- and α, β-band transitions are known. It is reasonable to assume that the axes of the Raman tensor and those of the optical absorption ellipsoid are the same, as they are both determined by the same dipole matrix elements.

According to Eaton and Hofrichter (1981)

$$\varepsilon_b/\varepsilon_a = \frac{1 - n_{zb}^2}{1 - n_{za}^2}, \tag{12}$$

where (n_{zb}, n_{za}) are the directional cosines of the z-axis of the Raman tensor with respect to the crystal axes, a, b, c^*, and

$$\varepsilon_c/\varepsilon_b = \frac{1 - n_{zc}^2}{1 - n_{zb}^2}, \tag{13}$$

with (n_{zb}, n_{zc}) directional cosines of the z-axis with respect to a^*, b, c axes of the crystal, where a^*- and c-axes are obtained by rotating the a- and c^*-axes, respectively by 15.78° around the b-axis (Phillips 1980). From these equations and $\sum_L n_{zL}^2 = 1$, $L = a, b, c^*$, we calculate the directional cosines of the z-axis.

The directions N_A-N_C and N_B-N_D may now be used as first approximations for the x- and y-axes. It turns out, however, that the directional cosinus n_{xa} varies in value between -0.06 and -0.168 within the error limits of this first approximation. The values n_{xb}, n_{xc^*} are in the order of 1 and change by only about 10%. Thus the value n_{xa} determines critically the matrix elements a_{xXkM} and a_{kMxX}.

We therefore choose the following procedure. The z-axis is calculated from the dichroic ratios $\varepsilon_c/\varepsilon_b$ and $\varepsilon_b/\varepsilon_a$ in the corresponding crystals. The value of n_{xa} is left variable within the limits determined above.

Once the value of n_{xa} and the direction of the z-axis is chosen the unknown values n_{iL} can be calculated.

Using these values and the values of β_{ik} as determined from the solution, the excitation profiles $|\beta'_{LM}|^2$ can be calculated by Eq. (7).

The value of n_{xa} is varied until best agreement to the experimental data is obtained.

To obtain the dichroic ratios we have measured the absorption coefficient ε_a, ε_b on the a, b face of a crystal with a microphotometer as described by Eaton and Hofrichter (1981). The ε_b and ε_c were measured also on crystal with b, c face.

The data for MbCN agree with those already published by Eaton and Hochstrasser (1981).

The value of $\varepsilon_c/\varepsilon_b$ taken from Eaton and Hochstrasser (1981) at the maximum of the Soret band is 1.26 ± 0.02. This value is also obtained in the region between the Q- and B-bands. For the value $\varepsilon_b/\varepsilon_a$ no data in the literature are given. The result of our measurement in the region between the Q- and B-band is $\varepsilon_b/\varepsilon_a = 2.85 \pm 0.05$.

For *deoxy*Mb we obtain from the maximum of the Q_v-band $\varepsilon_c/\varepsilon_b = 1.22 \pm 0.02$ and $\varepsilon_b/\varepsilon_a = 3.7 \pm 0.05$.

Figure 5 shows the measured optical density of *deoxy*Mb crystals with *a, b* face as a representative example.

From these data the directional cosines of the z-axis with respect to the crystal axis *a, b, c** are

for MbCN $n_{za}^2 = 0.723$, $n_{zb}^2 = 0.206$, $n_{zc}^2 = 0.071$
and for *deoxy*Mb $n_{za}^2 = 0.78$, $n_{zb}^2 = 0.18$, $n_{zc}^2 = 0.04$.

With these values of the z-direction and adjusting n_{xa} within the limits of variation we have calculated the excitation profiles of the crystals.

For $n_{xa} = -0.12$ in MbCN and $n_{xa} = -0.06$ in *deoxy*Mb the excitation profiles of the crystal agree to the experimental data (Figs. 1–4). This shows that the set solution data is sufficient to determine the Raman tensor with satisfying accuracy and confirms the method of Schweitzer et al. (1984). Further-

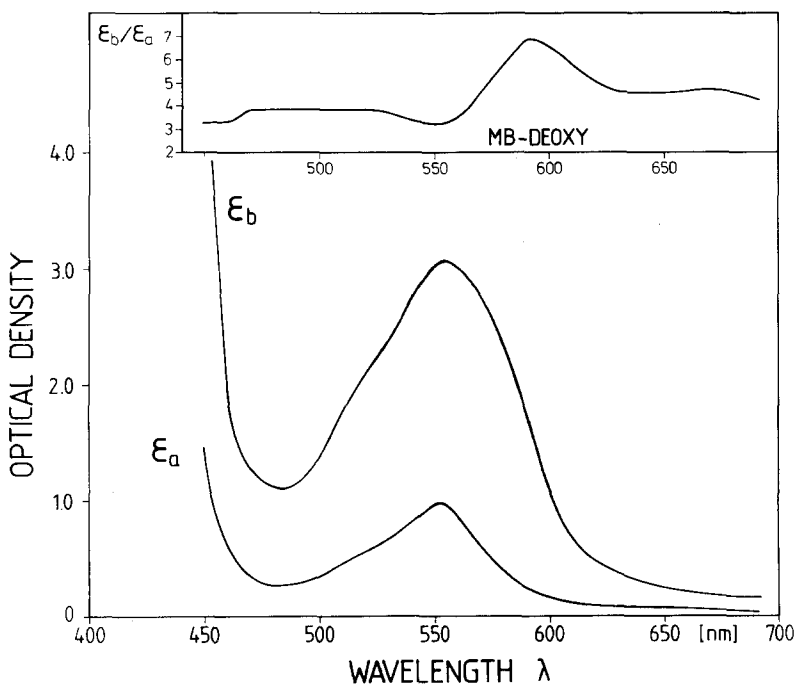

Fig. 5. Optical density of *deoxy*Mb single crystal. ε_a and ε_b are the optical density with light polarized parallel to the *a, b*-axis, respectively. The *upper curve* represents the polarization ratio $\varepsilon_b/\varepsilon_a$

more, we may draw the conclusion that in Mb the configuration of the haem plane in the crystalline state is identical to that of the molecule in solution.

From the values of the z-direction of both crystals one may conclude the upon ligation with CN the z-axis of the Raman tensor is shifted by an angle of 5° ± 2° with respect to the z-axis of the deoxy-state. Furthermore the x- and y-axis of the ligated state is shifted by a rotation about the z-axis by about 5° ± 2° with respect to the deoxy-state.

c) Discussion of the Symmetry-Classified Distortions

Table 1 lists the parameters that have been used to obtain the *deoxy*Mb fit.

For the line at 1,355 cm^{-1} only tensors of type A_{1g} and B_{2g} contribute. Since in D_{4h} this line is of A_{1g}-type, this contribution can be asserted to A_{1g} and B_{2g}-distortions (Schweitzer 1984). The line at 1,564 cm^{-1} shows contribu-

Table 1. Fitting parameters for the two Raman lines in *deoxy*Mb and ferric MbCN, respectively. The values are in arbitrary units related to the arbitrary units of Figs. 1–4. α_{es}^{Γ} and C_{es} see text, γ^{Q} and γ^{B} are the half-widths of the optical absorption of the Q- and B-bands. $\tilde{\nu}_{\mu}$ energy of the phonon to vibronic B- and Q-sidebands

Fit parameters		*Deoxy*Mb		Ferric MbCN	
		1,355 cm^{-1}	1,564 cm^{-1}	1,373 cm^{-1}	1,580 cm^{-1}
$\alpha_{QQ}^{A_{1g}}$	Re	−0.68	–	−3.5	–
	Im	2.3	–	–	–
$\alpha_{BB}^{A_{1g}}$	Re	1.4	3.2	6.48	0.33
	Im	7.48	3.2	8.425	6.7
$\alpha_{QB}^{A_{2g}}$	Re	–	2.48	−1.3	2.16
	Im	–	8.3	0.13	9.25
$\alpha_{QB}^{B_{1g}}$	Re	–	–	−3.4	–
	Im	–	–	−2.8	–
$\alpha_{QQ}^{B_{2g}}$	Re	1.7	3.8	–	2.16
	Im	–	−1.9	–	−4.5
$\alpha_{QB}^{B_{2g}}$	Re	0.88	–	0.26	–
	Im	–	–	2.3	–
$\alpha_{BB}^{B_{2g}}$	Re	1.6	3.36	–	–
	Im	–	−1.23	–	–
γ^{Q} (cm^{-1})		900	900	950	950
γ^{B} (cm^{-1})		1,900	1,900	1,870	1,870
$\tilde{\nu}_{\mu}$		1,440	1,440	1,430	1,500
C_{QQ}		0.003	0.01	0.003	0.01
C_{QB}		0.039	–	0.04	–
C_{BB}		0.004	0.004	0.004	–
$C_{QB}^{\tilde{}}$		0.039	0.04	0.04	–

tions from A_{1g}, A_{2g}, and B_{2g}-tensors, which are due to A_{2g}, A_{1g}, and B_{1g}-distortions, since in D_{4h} this line would be of A_{2g}-type. This seems to be contradictory, since the distortion should be independent of the observed lines. The electron-vibration-distortion coupling elements, however, do dependent on the representation of the Raman line, as has been discussed by Schweitzer (1983) in detail, and therefore one has to conclude that all distortions, i.e., A_{2g}, B_{1g}, and B_{2g} are present, lowering the symmetry of the molecule to C_s.

Table 1 lists the fitting parameters of ferric MbCN. For the line at 1,373 cm^{-1} contributions of all A_{1g}, B_{1g}, B_{2g}, and A_{2g}-tensors are present in contrast to *deoxy*Mb. This is plausible, since by insertion of the CN-ligand additional distortions are likely to arise. Since the bonding of CN influences mainly the central Fe^{3+} and the four nitrogen atoms of the pyrrol-ring a strong influence to A_{1g}-modes is excepted (Abe et al. 1978). A_{2g}-modes, however, should be less sensitive because their normal mode is less influenced by coupling between Fe^{3+} and the pyrrol-N (Warshel 1977). Therefore, in the 1,580 cm^{-1}-A_{2g}-line we observe the same contributions as in the case of *deoxy*Mb.

One important point should be mentioned. From measuring DPR and EPS in solution, one is not able to discriminate between B_{1g}- and B_{2g}-tensor contributions, since both Raman tensors contribute only to the tensor invariant γ^2. The contribution of B_{1g}- and B_{2g}-tensors to the tensor component $|\beta'_{XY}|^2$, $|\beta'_{YX}|^2$ in the laboratory system, however, are significantly different. In other words, if one interchanges B_{1g} and B_{2g} in the fitting procedure completely different crystal EPS are obtained.

Furthermore, we find that the line-widths of the Q- and Soret bands obtained from the fitting procedure agree well to the observed ones in both *deoxy*Mb and ferric MbCN. All the coupling constants C_{es}, related to the overlap integral of the vibronic functions are small as one would expect.

The good agreement of the experimental data obtained from measurements of crystals to those calculated from the EPS and DPR of Mb-solution confirms the approach of Schweitzer et al. (1984) to the parametrization of the complex DPR dispersion curves.

Acknowledgements. We would like to thank Mr. G. Ankele for technical assistance and Mr. W. Spickermann from the Computer Center of the University of Wuppertal for good advice in relation to the fitting program of the CERN library.

References

Abe M, Kitagawa T, Kyogoku Y (1978) Resonance Raman spectra of octaethylporphyrinato-Ni (II) and meso-deuterated and ^{15}N substituted derivatives II. A normal coordinate analysis. J Chem Phys 69 : 4526–4534

Bennet JE, Gibson JF, Ingram DJE (1961) Electron resonance studies of haemoglobin derivatives II. Results for types A, B, C, D, and F myoglobin crystals. Proc R Soc Lond [A] 262 : 395–408

Bernstein FC, Koetzle TF, Williams GJB, Meyer EF, Brice MD, Rodgers JR, Kennard O, Schimanochi T, Tajumi M (1977) The protein data bank: A computer-based archival file for macromolecular structures. J Mol Biol 112 : 535–542

Churg AK, Makinen MW (1978) The electronic structure and coordination geometry of the oxyheme complex in myoglobin. J Chem Phys 68 : 1913–1925

Collins DW, Fitchen DB, Lewis A (1973) Resonant Raman scattering from cytochrome c: Frequency dependence of the depolarization ratio. J Chem Phys 59 : 5714–5719
Damen TC, Porto SPS, Tell B (1966) Raman effect in zinc oxide. Phys Rev 142 : 570–574
Eaton WE, Hochstrasser RM (1968) Single-crystal spectra of ferrimyoglobin complexes in polarized light. J Chem Phys 49 : 985–995
Eaton WA, Hofrichter J (1981) In: Antonini E, Rossi-Bernardi L, Chiancone E (eds) Methods in enzymology, vol 76, chapt 76. Academic Press, New York London
Gouterman M (1959) Study of the effects of substitution on the absortion spectra of porphin. J Chem Phys 30 : 1139–1150
Kendrew JC, Parrish RG (1956) The crystal structure of myoglobin III. Sperm-whale myoglobin. Proc R Soc Lond [A] 238 : 305–324
Loudon R (1965) Theory of the resonance Raman effect in crystals. J Phys 26 : 677–683
Loudon R (1979) Quantum theory of light. Clarendon Press, New York
McClain WM (1971) Excited state symmetry assignment through polarized two-photon absorption. Studies of fluid. J. Chem Phys 55 : 2789–2796
Peticolas WL, Nafie L, Stein P, Fanconi B (1970) Quantum theory of the intensities of molecular vibrational spectra. J Chem Phys 52 : 1576–1588
Phillips SEV (1980) Structure and refinement of oxymyoglobin at 1.6 Å resolution. J Mol Biol 142 : 531–554
Placzek G (1934) Rayleighstreuung und Ramaneffekt. In: Marx E (Hrsg) Handbuch der Radiologie, Bd 6. Akademische Verlagsanstalt, Leipzig
Schweitzer R, Dreybrodt W, Mayer A, el Naggar S (1982) Influence of the solvent environment on the polarization properties of resonance Raman scattering in haemoglobin. J. Raman Spectrosc 13 : 139–148
Schweitzer R (1984) Untersuchung von pH-induzierten Symmetrieverzerrungen der prosthetischen Gruppe im Hämoglobin durch resonante Ramanstreuung. Dissertation, University of Bremen
Schweitzer-Stenner R, Dreybrodt W, el Naggar S (1984) Investigation of pH-induced symmetry distortions of the prosthetic group in deoxyhaemoglobin by resonance Raman scattering. Biophys Struct Mech 10 : 241–256
Sushchinskii MM (1972) Raman spectra of molecules and crystals. Israel Program for Scientific Translations, New York Jerusalem London
Warshel A (1977) Energy-structure correlation in metalloporphyrins and the control of oxygen binding by hemoglobin. Proc Natl Acad Sci USA 74 : 1789–1793
Watson HC (1969) The stereochemistry of the protein myoglobin. In: Harris and Aylett (eds) Progress in stereochemistry. Butterworths, London, pp 299–333

Received September 20, 1983/Accepted December 19, 1983